JACS
JOURNAL OF THE AMERICAN CHEMICAL SOCIETY

COMMUNICATION

pubs.acs.org/JACS

The Quest for Modular Nanocages: tbo-MOF as an Archetype for Mutual Substitution, Functionalization, and Expansion of Quadrangular Pillar Building Blocks

Jarrod F. Eubank,[†] Hasnaa Mouttaki,[†] Amy J. Cairns,[‡] Youssef Belmabkhout,[‡] Lukasz Wojtas,[†] Ryan Luebke,[‡] Mohamed Alkordi,[‡] and Mohamed Eddaoudi*[,†,‡]

[†]Department of Chemistry, University of South Florida, 4202 East Fowler Avenue (CHE 205), Tampa, Florida 33620, United States

[‡]KAUST Advanced Membranes and Porous Materials Center, 4700 King Abdullah University of Science and Technology, Thuwal 23955-6900, Kingdom of Saudi Arabia

Supporting Information

ABSTRACT: A new blueprint network for the design and synthesis of porous, functional 3D metal−organic frameworks (MOFs) has been identified, namely, the **tbo** net. Accordingly, **tbo**-MOFs based on this unique (3,4)-connected net can be exclusively constructed utilizing a combination of well-known and readily targeted $[M(R\text{-}BDC)]_n$ MOF layers [i.e., supermolecular building layers (SBLs)] based on the edge-transitive 4,4 square lattice (**sql**) (i.e., 2D four-building units) and a novel pillaring strategy based on four proximal isophthalate ligands from neighboring SBL membered rings (i.e., two pairs from each layer) covalently cross-linked through an organic quadrangular core (e.g., tetrasubstituted benzene). Our strategy permits the rational design and synthesis of isoreticular structures, functionalized and/or expanded, that possess extra-large nanocapsule-like cages, high porosity, and potential for gas separation and storage, among others. Thus, **tbo**-MOF serves as an archetypal tunable, isoreticular MOF platform for targeting desired applications.

Metal−organic frameworks (MOFs) are a burgeoning class of functional solid-state materials that are already being explored for use in multiple areas ranging from catalysis to surface chemistry, hydrogen storage, and carbon capture.[1] These promising materials are attractive to scientists in academia and industry alike because of their unique and readily functionalizable structures. In other words, their design and construction can be directed toward a targeted use: certain MOFs can be designed as platforms with controlled pore size, shape, and functionality for specific applications. To achieve framework design, however, a high degree of predictability must be integrated prior to synthesis, and it is still an ongoing challenge to absolutely predict the network topology of the constructed MOF.[2] To address this, our group has devoted its efforts to pinpointing particular blueprint frameworks that underpin our design strategies (preferably based on singular, exclusive nets for a combination of specific building blocks[3]) and are amenable to isoreticular chemistry.[2,4]

Edge-transitive nets are an obvious choice because they are typically the most appropriate targets in crystal chemistry and are suitable for the practice of reticular chemistry.[5] A given augmented net can be deconstructed into its basic building units, which are equivalent to vertex figures of the parent net (e.g., triangles for 3-connected nodes and squares for 4-connected nodes).[6] The generated (obtained) geometrical information is then employed to determine, design, and target prospective molecular building block (MBB) counterparts.[7] That is, such building units, as geometric entities, dictate the points of extension of the desired MBBs. The preferred MBBs can then be targeted by a combination of organic ligand synthesis and controlled metal−ligand-directed coordination.[8] The latter is the determining and critical factor in the successful practice of isoreticular chemistry, since access to precise reaction conditions is necessary for consistent generation of the inorganic MBB in situ.[2]

In our continuing quest to develop new strategies necessary for the rational assembly of MOF platforms, particularly those containing tunable cages (i.e., confined spaces) and readily amenable to isoreticulation, we re-examined augmented three-dimensional (3D) edge-transitive nets.[3] The deliberate intent was to identify hierarchal building units[2,9] (i.e., periodic 0D, 1D, or 2D building units[10]) containing elaborate, inbuilt structural information that is preferably distinctive to the given deconstructed parent augmented net. It should also be mentioned that interconnected cages are of interest because of their great importance for many applications, as has been observed in application-rich zeolites.[10]

We successfully implemented this strategy when we introduced the supermolecular building block (SBB) approach,[2] wherein sophisticated hierarchical construction information is embedded into the building unit(s), to deliberately assemble in situ a metal−organic polyhedron (MOP) with 24 additional, peripheral functional moieties (i.e., 24 points of extension) that, when combined with triangular building units, can exclusively assemble into a singular (3,24)-connected net, **rht**,[3] having extra-large cages.

During our quest, we recognized another distinctive net, **tbo-a**,[3] that exhibits explicit features of a potential blueprint net for logical design and directed assembly of MOF platforms. Uniquely, the **tbo-a** net is composed of 2D periodic arrays of squares, each consistent with an augmented 4,4 square grid or lattice (**sql-a**),[3] that are cross-linked through 4-connected (quadrangular) pillars (Figure 1b) and encompass inherent polyhedral cavities. The **sql-a** net, as one of only two edge-transitive 2D nets based on the assembly of squares,[3] is more easily attained in crystal chemistry. In fact, MOFs having **sql** topology based on

Received: June 17, 2011
Published: August 05, 2011

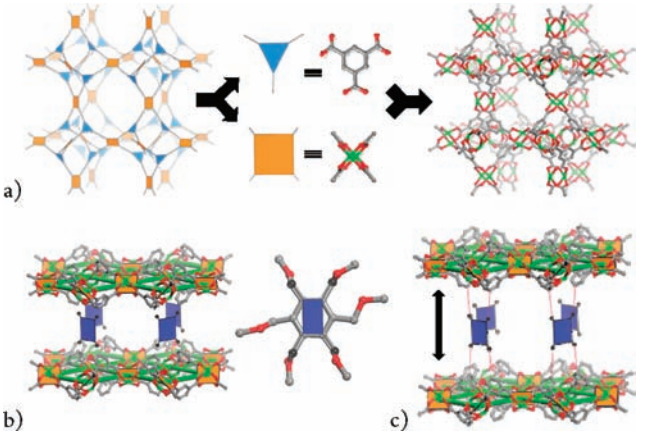

Figure 1. (a) Substitution of the vertex figures in the augmented **tbo** network, **tbo-a**, with analogous chemical entities results in a **tbo**-MOF. (b) **tbo**-MOFs can be targeted from **sql** SBLs (green) linked by 4-connected core pillars (blue), which can be functionalized. (c) Extension of the ligand between the core (blue) and the BDC results in a greater distance between the SBLs and increased confined space.

square paddlewheel dimer MBBs $[M_2(O_2CR)_4(A)_2$; M = metal, A = axial ligand] bridged by ditopic organic ligands [e.g., benzenedicarboxylates (BDCs) such as terephthalate or isophthalate] are well-known and readily constructed.[8,11] Thus, surface-decorated **sql**-MOFs (e.g., $[M(R\text{-}BDC)]_n$) could be employed as supermolecular building layers (SBLs)[11b] amenable to pillaring[12] via cross-linking through 4-connected organic building blocks to construct the desired **tbo**-MOF platform. The ability to generate $[M(R\text{-}BDC)]_n$ SBLs consistently in situ and space them using organic quadrangular pillars would permit the relatively small four-membered-ring (4MR) windows of the SBLs to be preserved, prohibiting self-interpenetration, while functionalizing and/or unilaterally enlarging the intrinsic confined space (e.g., distinct cages) delimited by the quadrangular pillars. This would permit access to made-to-order MOFs and exploitation of their resultant functionalized nanocages.

To implement our design strategy, we designed and synthesized the octacarboxylate ligand 5,5′,5″,5‴-[1,2,4,5-phenyltetramethoxy]tetraisophthalate (L1; Figure 2a) wherein an ether linkage was chosen to allow flexibility of the pendant BDC arms positioned in a squarelike geometry and retain their ability to freely form the intended SBL (**sql**-MOF). As expected, reactions of quadrangular-core tetra-BDC ligand L1 with Cu permitted the construction of the desired **tbo-a** framework, in which the **sql**-MOF SBLs are bridged by the organic quadrangles. Solvothermal reaction between the rectangle-like H_8L1 and $Cu(NO_3)_2 \cdot 2.5H_2O$ in an *N*,*N*-dimethylformamide (DMF)/water solution yielded a homogeneous crystalline material whose purity was confirmed by similarities between the experimental and calculated powder X-ray diffraction (PXRD) patterns (Figure S3 in the Supporting Information). The as-synthesized compound was characterized by single-crystal XRD as $[Cu_4L1(H_2O)_4 \cdot (solvent)]_n$ (**1**).

The resulting MOF can be viewed as a pillared **sql**-MOF based on L1 cores substituting the interlayer quadrangles and essentially pillaring 2D Cu-(5-R-isophthalate) **sql** SBLs. Thus, the quadrangular-pillared **sql**-MOF can be viewed as a 3D MOF wherein each L1 core serves as a 4-connected node, each 5-R-isophthalate moiety as a 3-connected node, and each $Cu_2(O_2CR)_4$ paddlewheel cluster as another 4-connected node. Topological analysis of the resultant (3,4)-connected net reveals that the topology of **1**

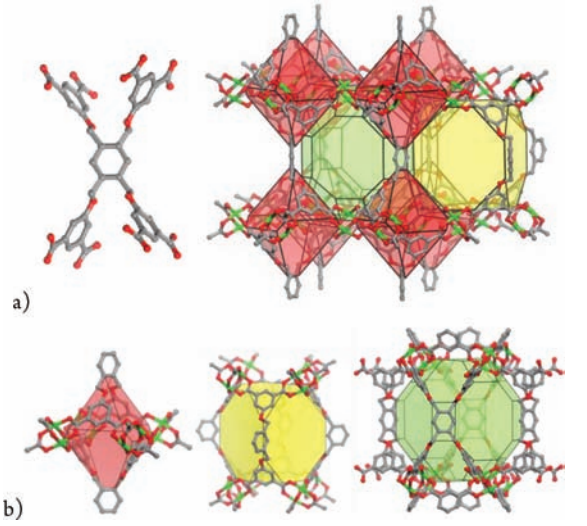

Figure 2. (a) (left) L1 ligand with tetraisophthalate groups connected via alkoxy links to a 4-connected benzene core. (right) Representative section of the crystal structure of **1** showing the polyhedral cages. (b) Three types of polyhedral cage in **1**: truncated tetrahedron (red), truncated cube (yellow), and truncated cuboctahedron (green).

corresponds to the expected **tbo**,[3] that is, **1** can be considered as a **tbo**-MOF (analogous to one prototypical MOF, HKUST-1[13]).

Alternatively, **1** can be interpreted as a MOF consisting of polyhedral cages[2,14] (Figure 2a), specifically face-sharing truncated cuboctahedra[3] [24 functionalized isophthalate ligands connected by eight $Cu_2(O_2CR)_4$ centers and four L1 benzene cores]. Each inorganic paddlewheel MBB is dinuclear and consists of two copper ions with the expected CuO_5 square-pyramidal geometry, with each Cu coordinated to four oxygen atoms of four carboxylates and one axial water molecule. Each carboxylate moiety of the octuply deprotonated L1 ligand coordinates in a bis-monodentate fashion to two Cu atoms, forming the $Cu_2(O_2CR)_4$ MBBs. The packing of these face-shared (through 4MRs) truncated cuboctahedral cages generates interpolyhedral cavities delineating two other cage types, truncated cubes and truncated tetrahedra (Figure 2b).

Thus, the overall neutral framework of **1** consists of three types of open cages (Figure 2b). The largest, truncated cuboctahedra having diameters of 17.787 and 18.349 Å [14.387 Å sphere including van der Waals (vdw) radii], are surrounded by six truncated cubes (Figure S2b) and eight truncated tetrahedra. The truncated cubes have diameters of 15.424 Å (height) and 16.102 Å (width) (12.024 Å vdw sphere) and are surrounded by six truncated cuboctahedra and eight truncated tetrahedra. The truncated tetrahedra have diameters of 12.521 Å (height) and 10.220 Å (width) (6.820 Å vdw sphere) and are surrounded by four truncated tetrahedra and four truncated cubes.

To confirm the efficacy of our design strategy, we functionalized ligand L1 with two extra pendant isophthalate arms (Figure 3a), which in principle could also potentially coordinate to metal cations and direct the formation of a different network (but only if the structure deviates from the targeted **sql** SBLs). To our satisfaction, the reaction of 5,5′,5″,5‴,5⁗,5⁗′-[1,2,3,4,5,6-phenylhexamethoxy]hexaisophthalic acid ($H_{12}L2$) with copper under reaction conditions similar to those for **1** yielded a MOF analogous to **1** wherein the two added pendant arms freely point into the generated cavities with no metal coordination.

dx.doi.org/10.1021/ja205658j |*J. Am. Chem. Soc.* 2011, 133, 14204–14207

Solvothermal reaction between rectangle-like H_{12}L2 and $Cu(NO_3)_2 \cdot 2.5H_2O$ in a DMF/water solution yielded a homogeneous crystalline material whose purity was confirmed by similarities between the experimental and calculated PXRD patterns (Figure S4). The as-synthesized compound was characterized by single-crystal XRD as $[Cu_4(H_4L2)(H_2O)_x(DMF)_{4-x} \cdot (solvent)]_n$ (**2**). As expected, the reaction gave the desired **tbo**-MOF, in which the necessary tetraisophthalate moieties are coordinated to Cu to form paddlewheels while the two extra isophthalates remain unbound and point into the large polyhedral cavities (Figure 3b).

Additionally, the uniqueness of our pillaring approach to **tbo**-MOFs should permit the construction of isoreticular MOFs with the same **tbo** topology via the expansion of the organic pillars, specifically by extension of the links between the quadrangular benzene core and the isophthalate moieties shown in Figure 1a, resulting in SBLs that are pillared and separated at a greater distance by the expanded quadrangles. To support this concept, we synthesized 5,5′,5″,5‴-[1,2,4,5-benzenetetrakis(4-methyleneoxyphenylazo)]tetraisophthalic acid (H_8L3), wherein the isophthalate moieties and benzene core of L1 were kept intact but the length between them was extended by using 4-hydroxyphenyl-1-diazene moieties as the links.

As projected, solvothermal reaction between H_8L3 and copper in a DMF/water solution afforded green crystals that were characterized by single-crystal XRD studies as $[Cu_4(L3)(H_2O)_3(DMF) \cdot (solvent)]_n$ (**3**), a 3D **tbo**-MOF isoreticular to **1** and **2**. The extra-large truncated cuboctahedral cages in **3** are more like nanocapsules (Figure 3c) and possess diameters in the mesoporous range (up to 29.445 Å × 18.864 Å and 26.045 Å × 15.464 Å including vdw radii). The truncated cubes have diameters of 28.682 Å (height) and 15.612 Å (width) (25.282 × 12.212 Å vdw), and the truncated tetrahedra have diameters of 26.499 Å (height) and 9.081 Å (width) (23.099 × 5.681 Å vdw).

The total solvent-accessible volumes of **1**, **2**, and **3** were estimated to be ∼72%, ∼56%, and ∼76%, respectively, by summing voxels more than 1.2 Å away from the framework using PLATON software.[15] Sorption studies performed on each compound confirmed their permanent porosity. Argon sorption experiments on compounds **1** and **2** gave fully reversible type-I isotherms (Figure S9) characteristic of microporous materials. The Langmuir apparent surface area of **1** was estimated to be 2896 m^2/g, which is higher than that of prototypical HKUST-1 (692−1944 m^2/g).[13,16] The calculated total free volume was estimated to be 0.97 cm^3/g. As anticipated, the effect of the ancillary pendant groups in compound **2** is reflected by the reduced surface area and free pore volume, which were estimated as 1490 m^2/g and 0.47 cm^3/g, respectively. Thus, isoreticular compounds **1** and **2** are attractive sorbents for evaluating the impact of pore size, shape, and functionality on the sorption energetics and uptake of industrially and environmentally relevant gases such as CH_4, H_2, and CO_2.

Accordingly, H_2, CO_2, and CH_4 sorption experiments were carried out at various temperatures and pressures. For H_2, the isosteric heat of adsorption (Q_{st}) was found to be higher for **2** than for **1** over the entire studied range (e.g., 7.6 vs 6.8 kJ mol^{-1} at low loading); nevertheless, the maximum uptake at 77 K and 1 bar was higher for **1** than for **2** (2.37 vs 1.80 wt %) (Figure S10). The observed improvement in the H_2 sorption energetics in the case of **2** is likely due to the combined size and surface effects of the exposed free carboxylic acids, which reduce the confined space and promote a localized higher charge density.[17] In the case of CO_2, it was anticipated that the free carboxylic acids exposed in the pores would enhance the energetics of CO_2 sorption; CO_2 is recognized to act as a Lewis base, leading to relatively strong specific interactions with carboxylic acids.[18] Indeed, the Q_{st} for CO_2 was found to be higher for **2** than for **1** over the entire studied range, with a more pronounced difference at low loading (35.2 vs 29.7 kJ mol^{-1}) (Figure 4a inset). It should be mentioned that at 258 K, the uptake was more pronounced for **2** than for **1** at reduced pressures; this trend was reversed once the uptake reached 8.5 mmol/mmol (at 1 bar, the maximum uptake was 10.1 for **1** vs 9.7 mmol/mmol for **2**) (Figure 4a).

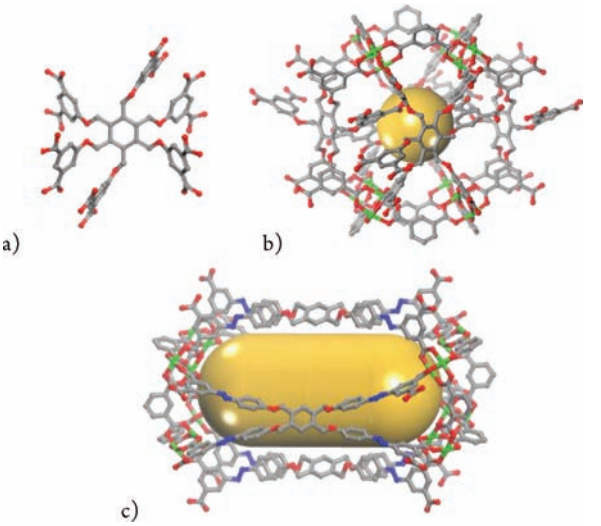

Figure 3. (a) Ligand L2, a functionalized version of L1. (b) Representation of the largest cage in **2**, in which the open space is reduced because of the pendant groups. (c) Representation of a nanocapsule cage in **3**. The vdw sphere in (b) and cylinder in (c) are shown in gold.

For further confirmation and elucidation of the impact of the free carboxylic acids on the CO_2 sorption energetics in the case of compound **2**, we elected to perform comparative sorption studies at room temperature and elevated pressures using a sorbate probe molecule without a quadrupole, namely, CH_4. In fact, a more pronounced difference between CO_2 and CH_4 uptake for **2** versus **1** was observed in the lower-pressure range (i.e., 0−5 bar) of the sorption isotherms (Figure 4b), indicative of enhanced CO_2 interactions with the framework, as also evidenced by the steepness of the CO_2 sorption isotherm at low loading for **2**. This result is in complete agreement with the relatively high Q_{st} observed at low loading for compound **2** versus **1**. It is worth mentioning that the CO_2 sorption isotherms at 298 K for **1** and **2** intersect at ∼6 bar and at an uptake (∼8.5 mmol/mmol) comparable to that observed in the sorption isotherms at lower temperature (258 K) (Figure 4a). Also, a noticeable difference in the CH_4 sorption isotherms was primarily observed only at higher pressures, which is likely correlated with the difference between the pore size distributions of compounds **1** and **2**, since CH_4-specific interactions with the free carboxylic acid groups are relatively less dominant than for CO_2. It is apparent that functionalizing the pores with moieties that can favorably interact with CO_2 should result in made-to-order MOFs with desired affinities and capacities for CO_2 capture and storage.

We have successfully adapted a modular pillaring strategy to the design and synthesis of isoreticular **tbo**-MOF platforms, including functionalization and expansion of cavities. The novel

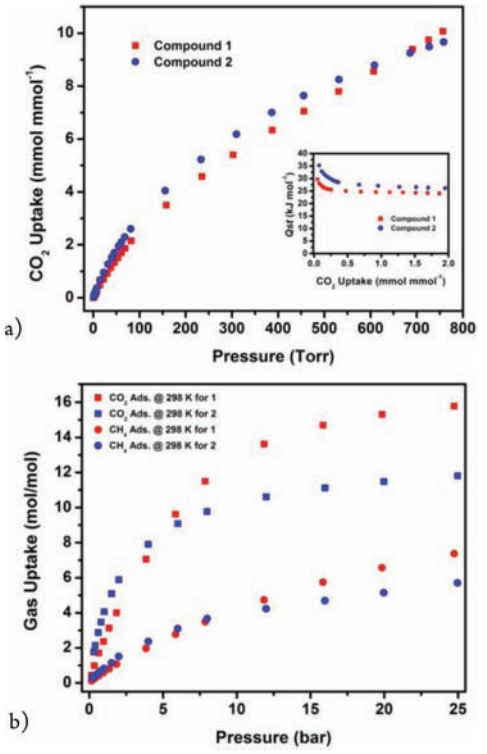

Figure 4. (a) CO_2 sorption isotherms for **1** and **2** at 258 K and (inset) isosteric heat of adsorption (Q_{st}) for CO_2 in **1** and **2**. (b) CO_2 and CH_4 high-pressure sorption isotherms for **1** and **2** collected at 298 K.

tbo-MOFs (i.e., quadrangular-pillared **sql**-MOFs) maintain thermal stability up to nearly 300 °C (Figures S7 and S8) and exhibit permanent porosities higher than those observed for the analogous HKUST-1 material. The addition of pendant functional groups, in this case carboxylic acids, enhances the affinity for guest molecules, particularly CO_2. Further sorption studies are underway to evaluate other potential guest molecules. Future work will include encapsulation of porphyrins and analogous molecules as well as corresponding catalytic studies. Also, the facile nature of MOF synthesis combined with our platform technique will allow us to integrate a variety of metals (e.g., Mo-, Fe-, and Cr-HKUST-1 analogues are already known,[19] and numerous metals are known to form the paddlewheel MBB[11a]). In addition, this approach based on pillaring of SBLs as the main periodic building units will permit the generation of MOFs with larger surface areas that can be readily functionalized prior the assembly process. Work is in progress to introduce various additional functionalities (e.g., various amines to evaluate their impact on CO_2 uptake) for targeted applications such as gas separation and development of thin-film-based MOFs.

■ ASSOCIATED CONTENT

Supporting Information. Experimental details, additional results, and crystallographic data (CIF). This material is available free of charge via the Internet at http://pubs.acs.org.

■ AUTHOR INFORMATION

Corresponding Author
mohamed.eddaoudi@kaust.edu.sa

■ ACKNOWLEDGMENT

This work is dedicated to the memory of I. Dale Shellhammer (1924−2010). The authors gratefully acknowledge funds from NSF (DMR 0548117) and KAUST as well as beamline 15ID-C of ChemMatCARS Sector 15 at APS, ANL (DOE DE-AC02-06CH11357, NSF CHE-0822838).

■ REFERENCES

(1) *Metal−Organic Frameworks: Design and Application*; MacGillivray, L. R., Ed.; Wiley-VCH: Weinheim, Germany, 2010 and references therein.
(2) Nouar, F.; Eubank, J. F.; Bousquet, T.; Wojtas, L.; Zaworotko, M. J.; Eddaoudi, M. *J. Am. Chem. Soc.* **2008**, *130*, 1833.
(3) O'Keeffe, M.; Peskov, M. A.; Ramsden, S. J.; Yaghi, O. M. *Acc. Chem. Res.* **2008**, *41*, 1782.
(4) Yaghi, O. M.; O'Keeffe, M.; Ockwig, N. W.; Chae, H. K.; Eddaoudi, M.; Kim, J. *Nature* **2003**, *423*, 705.
(5) (a) Delgado-Friedrichs, O.; O'Keeffe, M.; Yaghi, O. M. *Acta Crystallogr.* **2006**, *A62*, 350. (b) Delgado-Friedrichs, O.; O'Keeffe, M. *Acta Crystallogr.* **2009**, *A65*, 360.
(6) Ockwig, N. W.; Delgado-Friedrichs, O.; O'Keeffe, M.; Yaghi, O. M. *Acc. Chem. Res.* **2005**, *38*, 176.
(7) (a) Stein, A.; Keller, S. W.; Mallouk, T. E. *Science* **1993**, *259*, 1558. (b) Férey, G. *J. Solid State Chem.* **2000**, *152*, 37. (c) Eddaoudi, M.; Kim, J.; Rosi, N.; Vodak, D.; Wachter, J.; O'Keeffe, M.; Yaghi, O. M. *Science* **2002**, *295*, 469. (d) Kitagawa, S.; Kitaura, R.; Noro, S.-i. *Angew. Chem., Int. Ed.* **2004**, *43*, 2334.
(8) Tranchemontagne, D. J.; Mendoza-Cortes, J. L.; O'Keeffe, M.; Yaghi, O. M. *Chem. Soc. Rev.* **2009**, *38*, 1257.
(9) Sudik, A. C.; Cote, A. P.; Wong-Foy, A. G.; O'Keeffe, M.; Yaghi, O. M. *Angew. Chem., Int. Ed.* **2006**, *45*, 2528.
(10) Baerlocher, C.; McCusker, L. B. Database of Zeolite Structures. http://www.iza-structure.org/databases/ (accessed June 17, 2011).
(11) (a) Allen, F. H. *Acta Crystallogr.* **2002**, *B58*, 380. (b) Eubank, J. F.; Wojtas, L.; Hight, M. R.; Bousquet, T.; Kravtsov, V. Ch.; Eddaoudi, M. *J. Am. Chem. Soc.* [Online early access]. DOI: 10.1021/ja203898s. Published Online: June 15, 2011.
(12) Three basic types of pillaring: (a) Axial-to-axial: Ma, B.; Mulfort, K. L.; Hupp, J. T. *Inorg. Chem.* **2005**, *44*, 4912. (b) Ligand-to-ligand: Chen, B.; Ockwig, N. W.; Millward, A.; Contreras, D.; Yaghi, O. M. *Angew. Chem., Int. Ed.* **2005**, *44*, 4745. (c) Axial-to-ligand: see ref 11b.
(13) Chui, S. S. Y.; Lo, S. M. F.; Charmant, J. P. H.; Orpen, A. G.; Williams, I. D. *Science* **1999**, *283*, 1148.
(14) (a) Liu, Y.; Kravtsov, V. Ch.; Eddaoudi, M. *Angew. Chem., Int. Ed.* **2008**, *47*, 8446. (b) Sava, D. F.; Kravtsov, V. Ch.; Nouar, F.; Wojtas, L.; Eubank, J. F.; Eddaoudi, M. *J. Am. Chem. Soc.* **2008**, *130*, 3768. (c) Liu, Y.; Kravtsov, V. Ch.; Larsen, R.; Eddaoudi, M. *Chem. Commun.* **2006**, 1488. (d) Férey, G.; Mellot-Draznieks, C.; Serre, C.; Millange, F.; Dutour, J.; Surblé, S.; Margiolaki, I. *Science* **2005**, *309*, 2040.
(15) PLATON: (a) van der Sluis, P.; Spek, A. L. *Acta Crystallogr.* **1990**, *A46*, 194. (b) Spek, A. L. *Acta Crystallogr.* **1990**, *A46*, c34.
(16) Wong-Foy, A. G.; Matzger, A. J.; Yaghi, O. M. *J. Am. Chem. Soc.* **2006**, *128*, 3494.
(17) Liu, Y.; Eubank, J. F.; Cairns, A. J.; Eckert, J.; Kravtsov, V. Ch.; Luebke, R.; Eddaoudi, M. *Angew. Chem., Int. Ed.* **2007**, *46*, 3278.
(18) (a) Bell, P. W.; Thote, A. J.; Park, Y.; Gupta, R. B.; Roberts, C. B. *Ind. Eng. Chem. Res.* **2003**, *42*, 6280. (b) Torrisi, A.; Mellot-Draznieks, C.; Bell, R. G. *J. Chem. Phys.* **2010**, *132*, No. 044705.
(19) $Mo_3(BTC)_2$: Kramer, M.; Schwarz, U.; Kaskel, S. *J. Mater. Chem.* **2006**, *16*, 2245. $Fe_3(BTC)_2$: Xie, L.; Liu, S.; Gao, C.; Cao, R.; Cao, J.; Sun, C.; Su, Z. *Inorg. Chem.* **2007**, *46*, 7782. $Cr_3(BTC)_2$: Murray, L. J.; Dinca, M.; Yano, J.; Chavan, S.; Bordiga, S.; Brown, C. M.; Long, J. R. *J. Am. Chem. Soc.* **2010**, *132*, 7856.